Pramāṇa, Vol. 19, No. 4, October 1982, pp. 337–347. © Printed in India.

Design of an accelerating tube for electrostatic accelerators

P SINGH, T P DAVID and M G BETIGERI
Nuclear Physics Division, Bhabha Atomic Research Centre,
Bombay 400085, India

MS received 3 July 1982

Abstract. An accelerating tube has been designed and fabricated. Ion optical properties with different input beam geometries for 25 keV protons have been studied. An optimum voltage gradient in the first few sections required to obtain a focussed beam is determined. The tube has been installed in the 2 MV tandem accelerator built at Trombay and the performance of the tube is discussed.

Keywords. Accelerating tube design; trajectory calculations; tandem accelerating tubes; electrostatic accelerator.

1. Introduction

Accelerating tube forms an important component in electrostatic accelerators. Typically, the accelerating tube is an assembly of insulating rings and metal electrodes alternately stuck together to form an evacuated region for the ions to pass through. The metal electrodes are electrically connected to the corresponding equipotential planes in the voltage generator where a voltage gradient from high voltage terminal to the ground is established by means of a resistor chain. The ions injected into the tube, gain energy in each section corresponding to the voltage across the adjoining electrodes. The choice of the material for electrode is important to reduce electron loading caused due to passage of charged particles through the tube. Electrodes of aluminium, stainless steel and titanium metals have been reported in the literature. The shape of the electrode defines the fringing field in the entrance region and hence determines the ion optical properties of the tube. The focussing characteristics of a constant gradient accelerating tube made up of glass and aluminium electrodes have been reported by Rose *et al* (1964).

For the 2 MV tandem accelerator built at Trombay (Betigeri 1982), a low cost, strong focussing accelerating tube has been developed incorporating specially-shaped stainless steel electrodes. The shape of the electrode follows that of an intermediate electrode familiar in duoplasmatron ion sources where the shape is known to lead to a strong constriction of the plasma along the axis. Such a geometry is expected to lead to strong focussing in the entrance region so that a large variation in the input beam characteristics can be accepted. It is necessary to know the focussing properties of accelerating tube, especially in application to tandem accelerators where the first accelerating tube must focus the beam onto a narrow stripper canal in the terminal. The geometry used in the present design is shown in figure 1. Potential distributions subject to boundary conditions on the electrodes are obtained by solving Laplace

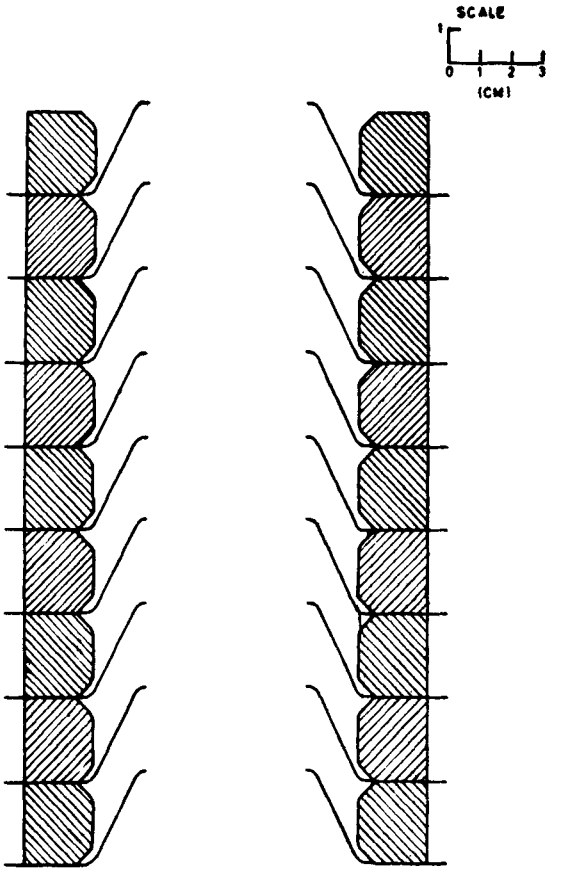

Figure 1. A typical section of the accelerating tube.

equation (§ 2). The calculations have been done for two sets of boundary conditions on the electrodes. In one set, the voltages on the first few electrodes are adjustable thus providing a varying potential gradient. In the second set a constant potential gradient of 40 kV per section is assumed. The trajectory calculations for the two sets of boundary conditions on electrodes are discussed in § 3. Two accelerating tubes, one for the low energy end and the other for the high energy end with 50 sections in each tube have been assembled for the 2 MV tandem accelerator. The details of assembly and the performance of the tube are discussed in § 4.

2. Potential calculations

For an accelerating tube with Z-axis along the tube, cylindrical symmetry exists. In such a case the potential distribution is given by

$$\frac{\partial^2 V}{\partial Z^2} + \frac{1}{r}\frac{\partial}{\partial r}\left(r\frac{\partial V}{\partial r}\right) = -4\pi\rho.$$

The term on the right side is due to space charge. The potential drop from the axis to the beam edge due to space charge (Wilson and Brewer 1973) arising out of 100 μA

proton beam is calculated to be 0·3 volt. Hence the effects due to space charge are neglected and the resulting Laplace equation (by equating the right hand term to zero in the above equation) is solved. The potential distribution in the desired region is numerically obtained by replacing Laplace's equation by a suitable difference formula. Details regarding the method of computation are given by Rose *et al* (1964). The present calculations differ from Rose *et al* (1964) only in the treatment of singularity at $r=0$. Using Hospital's rule the Laplace's equation can be written in the form

$$\frac{\partial^2 V}{\partial Z^2} + 2\frac{\partial^2 V}{\partial r^2} = 0,$$

which can be converted into a difference formula

$$V_{m+1,n} - 2V_{m,n} + V_{m-1,n} + 2(V_{m,n+1} - 2V_{m,n} + V_{m,n-1}) = 0.$$

The expression can be rewritten in view of the cylindrical symmetry as

$$V_{m,n} = \frac{V_{m+1,n} + V_{m-1,n} + 4V_{m,n+1}}{6}$$

The potential $V_{m,n}$ refers to the potential distribution in the plane (Z, r) at nodal points (mh, nh) in terms of a mesh spacing h.

A computer program TANDEM (Singh *et al* 1977) is used to calculate the potential at each point of the mesh. The electrode shape is approximated such that it lies on the mesh points. A mesh size of 1 mm is chosen so that electrode boundaries coincide with mesh lines thus avoiding the complexity of difference formulae for numerical solution near the boundary. The effect of this approximation is felt maximum near the electrode tips only. The iteration procedure is continued till the error $\epsilon = (V_{n-1} - V_n)/V_n$ becomes less than 0·008; here V_n and V_{n-1} are potentials at any point after nth and $(n-1)$th iterations respectively.

The program calculates potential at each point for two sets of boundary conditions on the electrodes. In one set, a varying potential gradient is established such that a singly charged particle gains an energy of 10 keV in the first two sections, 20 keV in the third section and later on 40 keV per section for the remaining tube (figure 2).

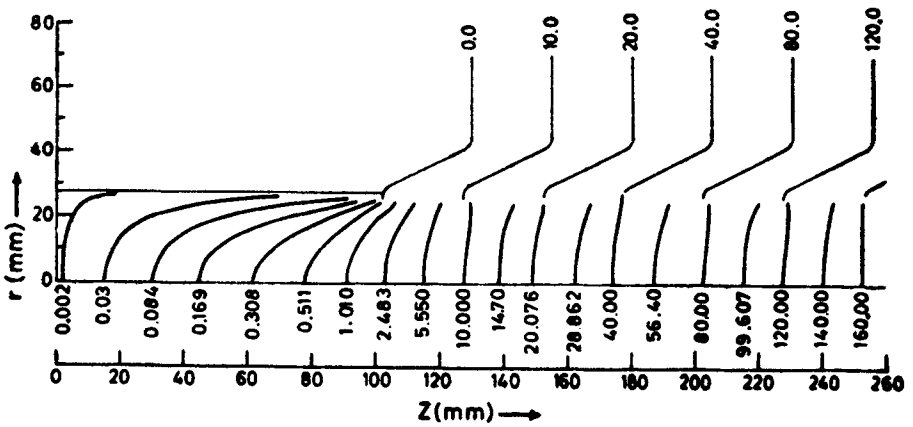

Figure 2. Potential distribution for the varying potential gradient case. Potentials are in kV.

In the second set, a constant potential gradient of 40 kV per section is assumed (figure 3). The origin of the coordinate system for the accelerating tube geometry has been fixed at 100 mm from the tip of the first electrode on the assumption that the ion beam can be focussed onto the origin by suitable voltage ratios of the electrodes of an Einzel lens. Therefore the beam entering the drift space between the origin and the grounded first electrode is diverging. The potential distributions obtained for the two sets of boundary conditions are shown in figures 2 and 3.

3. Trajectory calculations

The calculations of ion-trajectories in the accelerating tube involve solution of equations of motion of charged particles in electrostatic field:

$$F_Z = -e_i \frac{\partial V}{\partial Z}; \; F_r = -e_i \frac{\partial V}{\partial r}.$$

The exact formulation of the problem is given by Klemperer and Barnett (1971). A programme TANRAY (Singh *et al* 1977) has been used to trace ion trajectories for the two sets of boundary conditions on the electrodes mentioned before. The trajectories of 25 keV protons starting from $Z=0$ with different (r, θ) values corresponding to realistic input beam configurations have been calculated and are shown in figure 4 and figure 5 for the two sets of boundary conditions on the electrodes respectively. The effect of entrance region on a parallel beam ($Z=0$, $\theta=0$, different r's) has been studied in the case of the two potential distributions and are shown in figure 6 and figure 7 respectively. As expected, the focussing properties of the tube are mainly determined by the fringing field. It is to be noted that all trajectories do not cross the Z-axis at the same point in figures 6 and 7. Such a spread in focal lengths can be identified with the spherical aberration parameter familiar in the optical system. For paraxial rays the focal length increases with r (figure 8), which corresponds to negative spherical aberration for the accelerating tube. The results indicate that, in all respects, it is satisfactory to maintain varying gradient at the electrodes. The calculations indicate that the accelerating tube can handle large variations in the input beam emittance, but still leads to a focussed beam at the stripper canal.

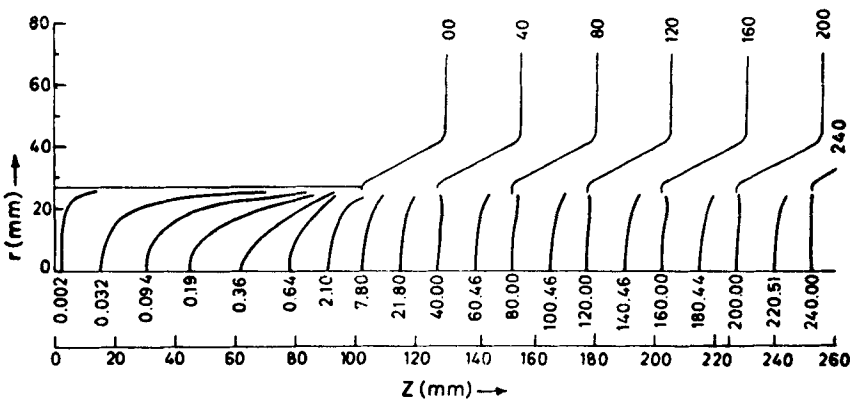

Figure 3. Potential distribution for the constant potential gradient case. Potentials are in kV.

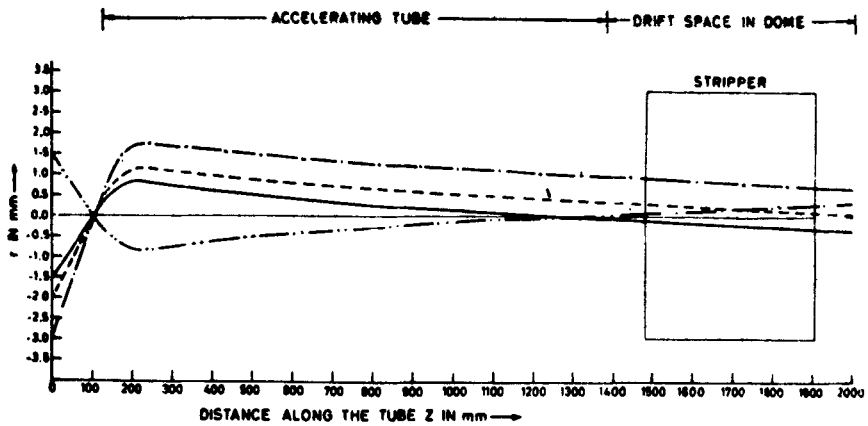

Figure 4. Trajectories for different input parameters (r, θ) of 25 keV protons in the case of varying potential gradient accelerating tube.

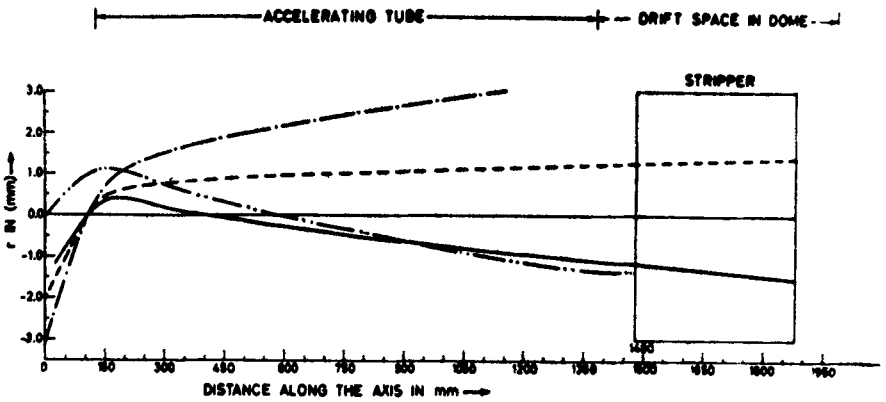

Figure 5. Trajectories for different input parameters (r, θ) of 25 keV protons in the case of constant potential gradient accelerating tube.

In a tandem accelerator, a beam of negatively-charged particles undergoes charge exchange process at the stripper canal in the terminal. The positively charged particles enter the second accelerating tube with higher incident energy than the particles entering the first tube and under the influence of an uniform electrostatic field, are accelerated to travel along a parabolic path. Under such an assumption, the ion trajectories are calculated using classical equations of motion. The calculations predict a circular cross-section of 1·4 mm diameter at the exit of the second tube for protons. For heavy ions, the trajectory calculations have been done for $A=40$ ions and the calculations predict a reduction in the size of the emergent beam as a function of the charge state (figure 9).

4. Construction and performance

The accelerating tubes for the 2 MV tandem accelerator consist of a periodic repetition of an 'Index' glass ring of dimensions, outer diameter 127 mm, internal diameter 82 mm, thickness 25 mm and a stainless steel electrode of dimensions outer diameter

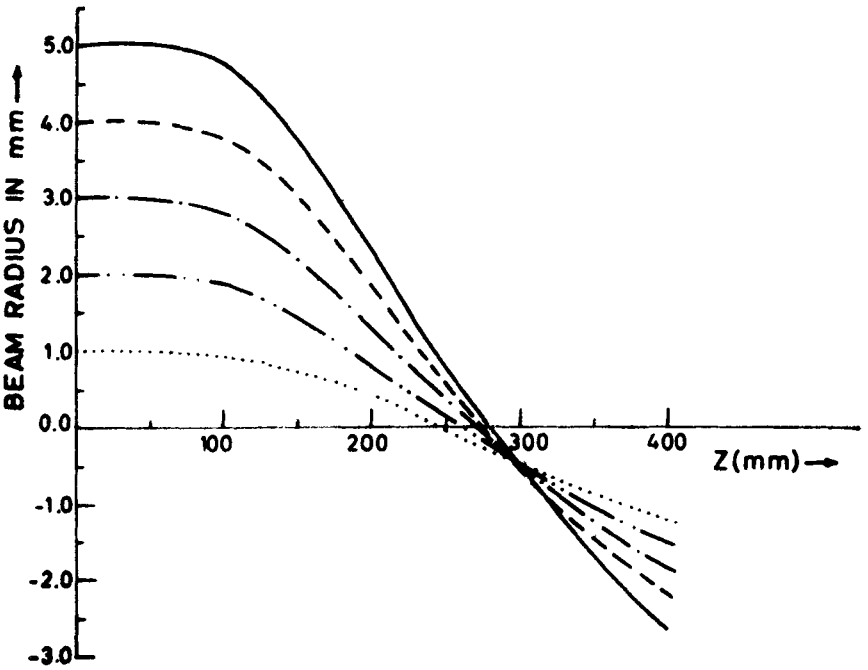

Figure 6. Trajectories of parallel beam of 25 keV protons in the entrance region for varying potential gradient case.

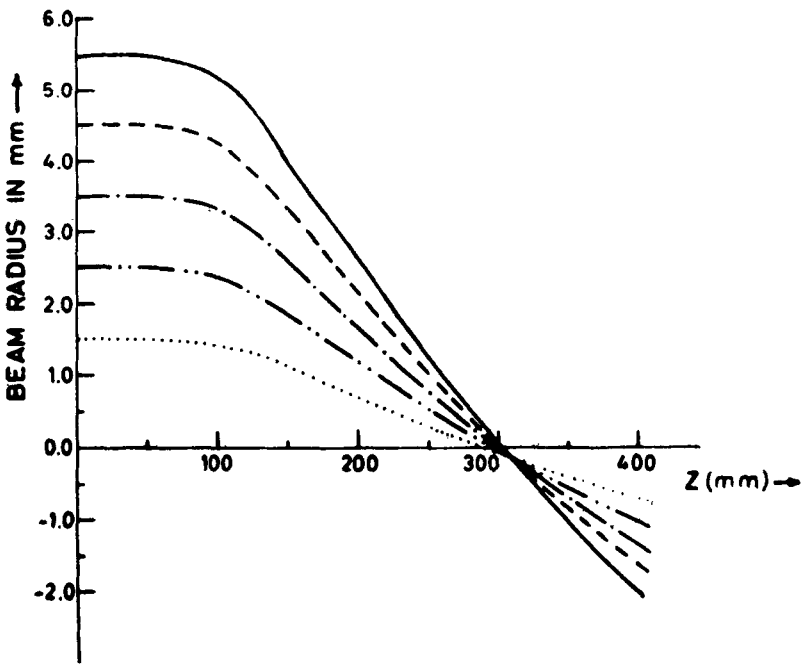

Figure 7. Trajectories of parallel beam of 25 keV protons in the entrance region for constant potential gradient case.

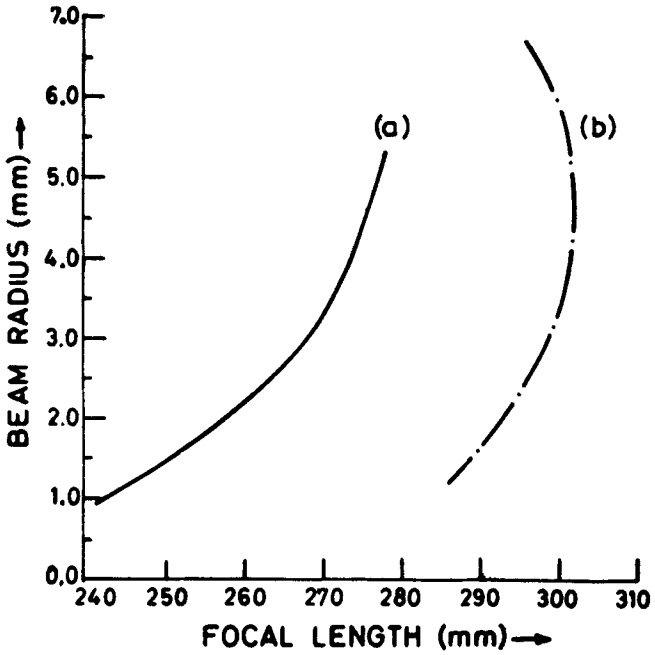

Figure 8. Focal length for parallel trajectories with different r's for (a) varying potential gradient case (b) constant potential gradient case (For discussion see text).

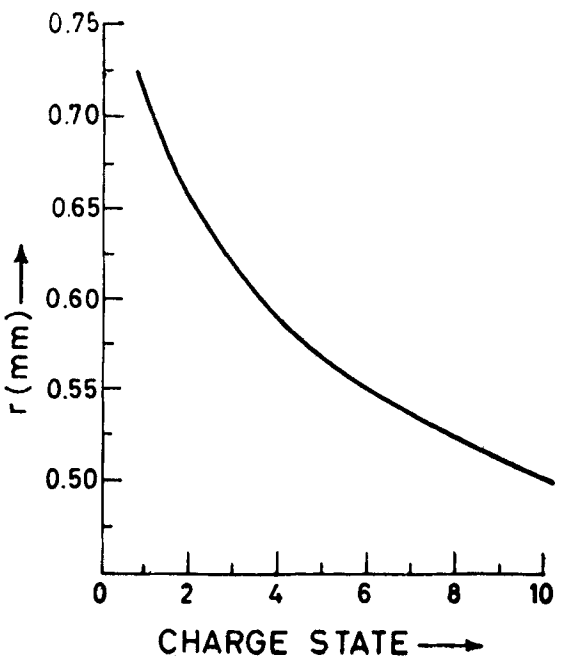

Figure 9. Beam radius of $A = 40$ ions (at the exit of the second tube) as a function of its charge state after stripper.

140 mm, internal diameter 50 mm, thickness 0·8 mm (figure 10) glued together with araldite. The 'index' glass used in the tube has been tested for surface leakage under controlled humidity condition (RH = (48 ± 5)% and temperature (25 ± 1)°C). The surface resistance was found to be ~8000 MΩ at 10 kV applied between the faces of the glass ring. The glass rings were also subjected to strong x-ray radiation in the terminal of 5·5 MV Van de Graaff continuously for 15 days. No change in resistivity and colour was noticed. The glass rings obtained from commercial sources had to be ground to ensure surface parallelism and thickness to an accuracy of ± 50 μ. The stainless steel electrodes were pressed out using special dies and buffed to mirror polish. The assembling of the stainless steel electrodes and glass rings was carefully done using jigs to ensure that the axis of the tube remains aligned. A set of 5 sections was araldited at a time the limit arising from the potlife time of the mixture of araldite and hardner. Such a subassembly, after it was allowed to set for 48 hours, was individually tested for an internal pressure of 5×10^{-6} torr and an external gas pressure of 300 psi. Procedure for cleaning of the surfaces of electrode and glass section had to be strictly followed to ensure such a seal. The final assembly of 10 such subsections was done in one setting. Spark gaps were provided to protect the tube from excessive voltage surges. The accelerating tubes were mounted through bellows from the two end flanges of the tank (figure 11). The final alignment of tubes and the stripper canal using He-Ne laser required slight adjustment of the bellows. The tubes are evacuated using two 2000 l/sec diffusion pumps on either side backed by a 800 l/sec vapour booster pump and a 150 l/min rotary pump. Liquid nitrogen traps are provided on the pumps to avoid backstreaming oil vapours from settling on the inside surface of the tube.

Each electrode of the accelerating tube is connected to the corresponding equipotential plane in the voltage generator. A column current of 10 μA through 4000 MΩ resistor develops a uniform voltage gradient of 40 kV per section. The required resistance is obtained by connecting in series sixteen 250 MΩ resistors in a specially designed polystyrene box which is fitted diagonally between the adjoining column sections. Provision of varying gradient on the electrodes therefore required adjustment of the values of these resistors correspondingly.

Negative hydrogen ions at 25 keV were extracted directly from a duoplasmatron ion source. The beam passes through two Einzel lenses, one before the preselector magnet and the other one before injection into the tube. An intensity of 2·5 μA was measured before putting the beam into the tube. Oxygen gas was used as the stripper gas. The beam at the exit of high energy accelerating tube was measured without electron suppression. At 1·4 MV on the terminal a maximum of 40 nA, H^+ could be measured when the accelerating tube was operated in constant gradient mode. However, the transmission increased markedly when the varying gradient mode was established. Under similar conditions an intensity of 1·8 μA H^+ was measured. At the time of these measurements, the energy stabilization was not yet done and no analyser magnet was used. Subsequently, the analysing magnet has been installed. Energy analysed and corona stabilised proton and oxygen beams are now routinely available. At 1 MV terminal voltage, 200 nA of H^+ beam has been obtained. Oxygen beams of 18 nA, 30 nA and 3 nA corresponding to O^{+++}, O^{++} and O^+ charge states respectively have been obtained at 800 kV terminal voltage.

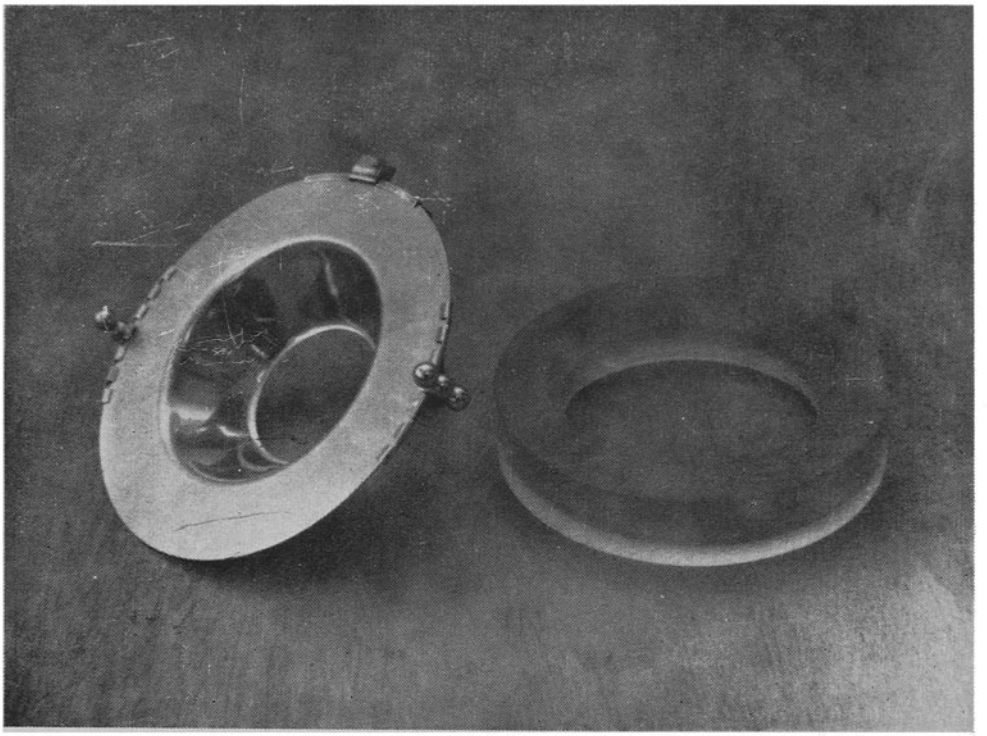

Figure 10. Glass ring and stainless steel electrode for accelerating tube.

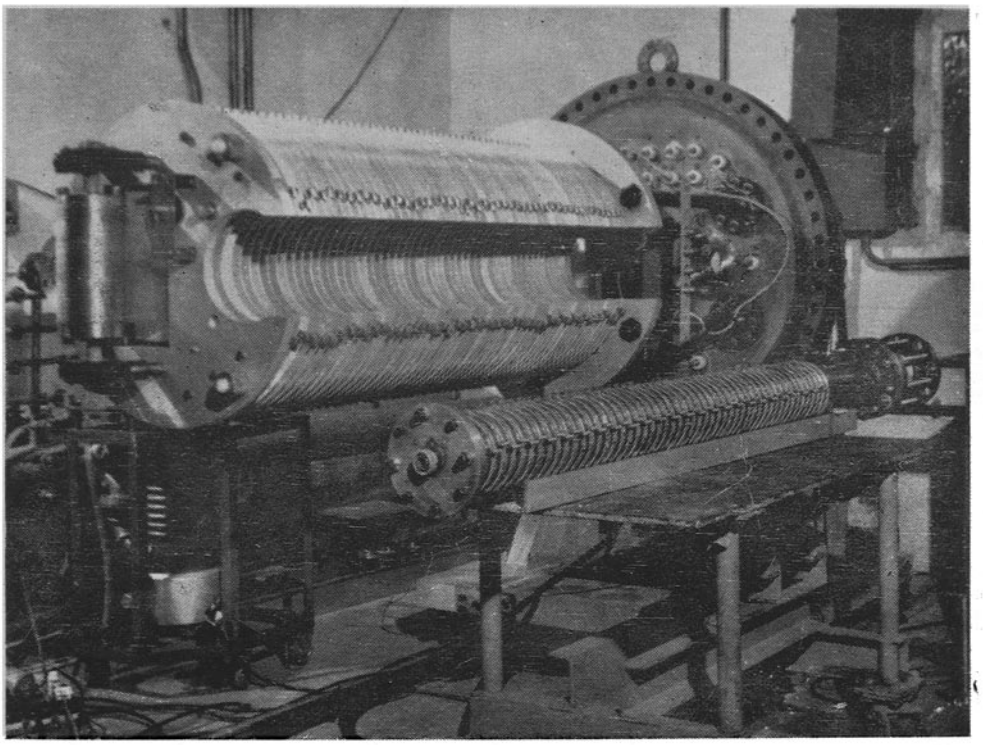

Figure 11. Accelerating tube assembly and the column structure.

Acknowledgements

The dies required for pressing stainless steel electrodes were machined at the Reactor Control Division workshops. We thank Shri C S Natarajan for fabricating the electrodes. We thank Shri J N Soni of Nuclear Physics Division workshop for fabricating various jigs and fixtures used in the assembly of the accelerating tube. We thank Dr A K Jain for useful discussion during the calculations. We are grateful to Shri D V Petkar and his colleagues in the Reliability Evaluation Laboratory for conducting the necessary tests on the Index glass rings used in the accelerating tube.

References

Betigeri M G, David T P, Hiremath S C, Iyengar P K, Mehta M K, Raju V S, Singh P and Soni J N 1982 Pramana **19**

Klemperer O and Barnett M E 1971 *Electron optics* (Cambridge: University Press) 3rd ed. pp. 473

Rose P H, Galejs A and Peck L 1964 *Nucl. Instrum. Meth.* **31** 262

Singh P, Jain A K, David T P and Betigeri M G 1977 BARC Report-934

Wilson G and Brewer R 1973 *Ion beams* (New York, USA: Wiley-Interscience) pp. 132.